High-temperature and high-pressure phase transitions in uranium

J. Bouchet and F. Bottin
CEA, DAM, DIF, 91297 Arpajon Cedex, France
(Received 24 November 2016; published 17 February 2017)

The phase diagram of uranium has been explored up to 100 GPa and 2000 K by means of *ab initio* molecular dynamics (AIMD) simulations. The lattice dynamics and energetics of the stable phases observed experimentally in this range of pressure and temperature are studied in this work. The phonon spectra of the α and γ phases are shown to evolve strongly as a function of temperature, unveiling the huge anharmonic effects present in this material. If the elastics constants and the bulk and shear moduli of the γ phase do not disclose any temperature effects, the shear modulus of the α phase decreases strongly as a function of temperature. Using the pressure- and temperature-dependent vibrational density of states and the Gibbs free energy of these two structures, we found a line transition between the α and γ phases which slightly underestimates the experimental one. Coherently with experiments, the bct structure is never found stable between 0 and 100 GPa.

DOI: 10.1103/PhysRevB.95.054113

I. INTRODUCTION

The actinides phase diagrams propose an incredible diversity of structures, not found elsewhere in the periodic table [1]. From Th to Pu, ground state structures exhibit increasing complexity. The series begins with the close-packed face centered cubic (fcc) structure for Th, followed by the body centered structure of Pa, and the orthorhombic structures of U and Np, to reach one of the most complex structures to be found for an element, to wit the monoclinic α phase of Pu. Thereafter, this tendency to condense in open structures ends abruptly, and elements beyond Pu adopt compact structures, e.g., dhcp (Am), or fcc (Cm).

The $5f$ electrons play a fundamental role in our understanding of these anomalous features. In light actinides, these electrons are itinerant, and contribute to bonding (as in the transition metals series), whereas after Pu they are localized and nonbonding (as in the rare earth series). Pressure has some remarkable effects on the electronic structure of the actinides, giving rise to a multiplicity of phase transitions [2]. In light actinides, pressure induces an electron transfer between the spd bands and the $5f$ band. As the number of f electrons increases, these elements take on the crystal structure of the element immediately to the right in the periodic table. Consequently, under compression, Th undergoes a phase transition from fcc to bct, the ground state structure of Pa, while Pa transforms to the α-U structure. Electrons starts to acquire delocalized character and participate in the bonding. As a consequence Am undergoes transitions to low symmetry crystal structures found in the light actinides series [3].

The behavior of the actinides in temperature is much less understood due to the difficulty to treat electronic and atomic degrees of freedom simultaneously in the calculations. The actinide series exhibits a strong variation of the melting temperature at room pressure, going from 2023 K for Th to 914 K for Pu. As with pressure, temperature also induces multiple phase transitions but all eventually lead to the same structure before the liquid, the body centered cubic (bcc) one. It is well known that this structure is mechanically unstable at room temperature, with a negative C' shear modulus [4]. Therefore, the thermal contributions as the vibrational entropy are certainly responsible for the stabilization of this structure at high temperature [5].

Density functional theory (DFT) has proved essential in drawing up this intelligible picture of the ground state properties of the actinides and their phase transitions in pressure [4,6–9]. At 0 K, phonon dispersions relations are nowadays routinely undertaken, thanks to the density functional perturbation theory (DFPT) [10]. This method has been applied to the ground state of Th [11] and U [12,13] with good agreement with neutron scattering data [14,15]. To study thermal properties, the quasiharmonic approximation (QHA) was applied with success for Th [11], but failed to reproduce the thermal behavior of the bulk modulus of α-U due to the presence of soft modes at low temperature [16]. For similar reasons, the high-temperature bcc structure of the actinides cannot be deduced from calculations performed at 0 K [17]. To overcome this inherent difficulty of the QHA, the temperature has to be directly included in the calculations. Using AIMD simulations and the temperature-dependent effective potential technique (TDEP) developed by Hellman and co-workers [18,19], we have recently reproduced the temperature evolution of the soft mode in α-U [20] while using the self-consistent *ab initio* lattice dynamics (SCAILD) technique. Söderlind *et al.*[17] have obtained stable phonon dispersions of γ-U at 1113 K.

The phase diagram of uranium has been studied experimentally by x-ray diffraction of a laser heated sample in a diamond anvil cell [21] up to 100 GPa. At ambient pressure, uranium is known to undergo two phase transitions: from the orthorhombic α to the bct β phase at 940 K and then to the bcc γ phase at 1050 K [1]. As a function of pressure, the bct phase disappears rapidly and an increasing line transition between the α/γ phase remains up to 100 GPa.

Here we propose to study the α/γ phase boundary of uranium up to 100 GPa. To reach this goal, we will compare the Gibbs free energy of the two structures at various pressures and temperatures obtained using AIMD and the TDEP method. We will also discuss the thermodynamic and the thermoelastic properties directly obtained from the phonon spectrum.

II. SIMULATION METHOD

Simulations were performed using the ABINIT package [22,23] in the framework of the projector augmented wave

(PAW) method [24,25] and by means of the generalized gradient approximation (GGA) according to the parametrization of Perdew, Burke, and Ernzerhof (PBE) for the exchange-correlation energy and potential [26]. Using ATOMPAW [27–29], we generated a PAW atomic data with a radius r_{PAW} equal to 1.51 Å, with $6s$, $6p$, $7s$, and $5f$ states as valence electrons. The cutoff energy chosen for the plane wave set along the AIMD simulations is equal to 435 eV.

The α-U structure was relaxed at 0 K for volumes corresponding to pressures between -10 and 100 GPa. The cell parameters obtained at each volume were used for the molecular dynamics simulations at 1000, 1300, 1600, and 2000 K, so no relaxation of the cell parameters in temperature is included in our simulations (we will discuss this approximation later in this paper). A $4 \times 2 \times 3$ α-U supercell including 96 atoms was used in the AIMD calculations with a $2 \times 2 \times 2$ Monkhorst-Pack mesh leading to the inclusion of four special **k** points. For the bcc structure, we used a $4 \times 4 \times 4$ supercell including 128 atoms with only the Γ point since it is sufficient to converge the vibrational free energies to 1 meV. We used the same volumes and temperatures as for the α phase. Simulations were performed in the NVT ensemble (constant number of particles, constant volume, and temperature) and were run for about 3 ps using a time step (τ) of 2.5 fs. Taking the benefit of an efficient scheme of parallelization [30] and using hundreds to thousands of processors, the recovery time is a few months.

To extract the vibrational frequencies from the AIMD simulations we used the TDEP technique developed by Hellman and co-workers [18,19]. In this method, a model Hamiltonian expanded in the harmonic form is used to fit the Born-Oppenheimer molecular dynamics potential energy surface at finite temperature and to obtain the interatomic force constants (IFCs). Once the IFCs are obtained, a Fourier transform is performed to get the dynamical matrix at any **q** point of the Brillouin zone. Taking into account the whole symmetries of the system, we have to calculate 50 coefficients for the α-U structure (up to the 11th shell of nearest neighbors) and 13 coefficients for the γ structure (up to the 6th shell of nearest neighbors).

III. RESULTS AND DISCUSSION

A. α phase

The phonon spectra of uranium has already been obtained at room temperature and up to 900 K using the TDEP method [20], see Fig. 1. When the temperature increases, the phonon frequencies are reduced, except for the soft mode observed in the middle of the [100] direction. This one increases as a function of the temperature and is responsible for the charge density wave (CDW) phase transition appearing at 50 K and leading to the α_1 structure [12,31]. Even at 900 K the softening is still clearly visible, showing that the thermodynamic properties are affected by the CDW at temperatures far above the phase transition. At ambient pressure, uranium transforms to the bct β phase at 940 K and then to the bcc γ phase at 1050 K [1]. We do not observe any softening in relation to these phase transitions in the α-U phonon spectra, meaning that they are not displacive phase

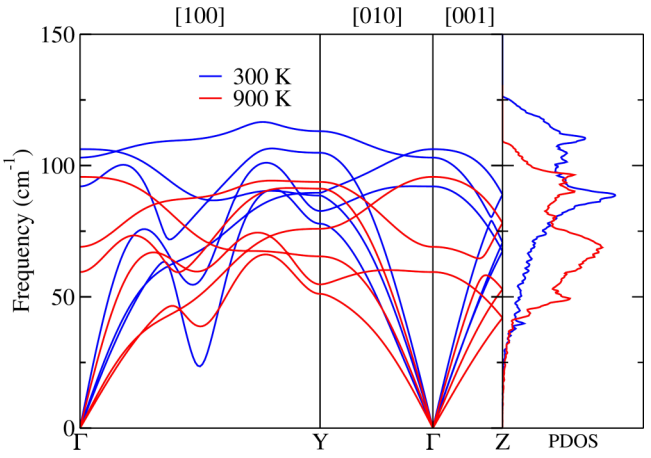

FIG. 1. Phonon dispersions and density of states for α-U at 300 and 900 K.

transitions but due to the competition between the vibrational entropies of the structures.

We show in Fig. 2 the phonon spectra of α-U at 19 and 88 GPa and at a temperature of 1600 K. Pressure strongly influences the CDW transitions in uranium which disappear at 2 GPa. At high pressure, the softening has almost completely disappeared and only a kink is visible in the phonon branch. As in temperature, we do not observe the appearance of soft modes with pressure, the phonon frequencies increase as a function of pressure. We found that the α-U structure is mechanically stable at all the volumes and temperatures considered here: up to 100 GPa and 2000 K.

At 1000 K we obtain an equilibrium volume of 21.2 Å^3 to be compared with the experimental value [32] of 21.7 Å^3. This difference between theory and experiment is of the same order as the one found at 0 K [12], 20.2 versus 20.6 Å^3. The thermal expansion of α-U is therefore well reproduced in AIMD simulations. From the phonon spectrum, it is straightforward to extract the sound velocities and calculate the elastic constants. We show in Fig. 3 the bulk and the shear moduli K and G as a function of pressure and for the four temperatures

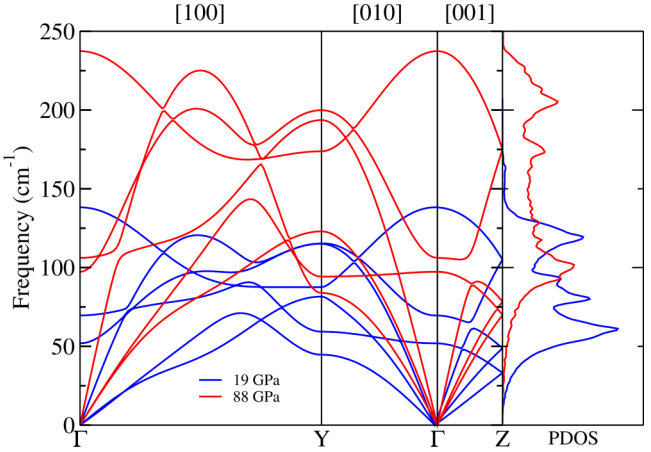

FIG. 2. Phonon dispersions and density of states for α-U at 19 and 88 GPa and 1600 K.

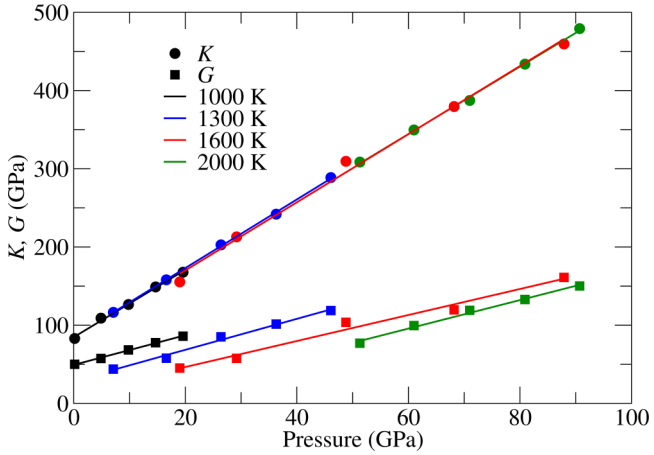

FIG. 3. Bulk modulus K and shear modulus G of α-U as a function of pressure and at several temperatures. The symbols are the calculated values and the lines are linear fits of these values.

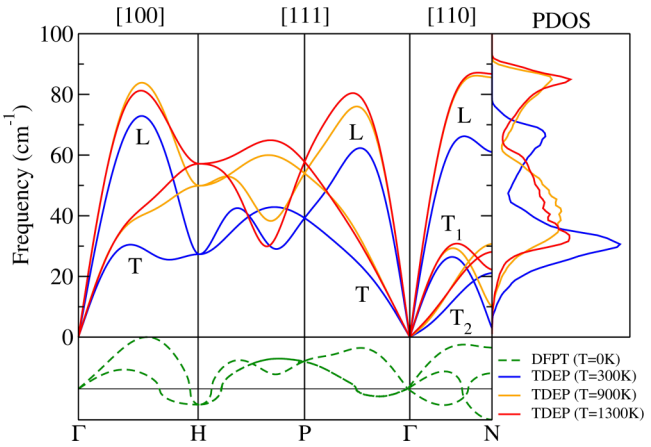

FIG. 4. Phonon dispersions and density of states for γ-U at 300, 900, and 1300 K using the TDEP method. The lower panel shows the phonon dispersions of γ-U at 0 K obtained with the DFPT method.

considered in this work (we used the Voigt average). At 1000 K and 0 GPa we found 85 and 50 GPa for K and G, respectively, while experimentally at 923 K the ultrasound data are 101 and 47 GPa [33]. The agreement is also remarkable for the compressional and the shear sound velocities V_p and V_s. At 1000 K, our calculations give $V_p = 2.82$ km s^{-1} and $V_s = 1.63$ km s^{-1}, while at 923 K, the experimental values [34] are 2.99 and 1.61 km s^{-1}. The evolution in pressure is linear for both modulus. Temperature has a different effect: K is almost constant between 1000 and 2000 K while G is strongly reduced (almost 50% between 1300 and 2000 K at 50 GPa).

B. γ phase

The bcc structure is the stable phase of uranium at temperatures from 1045 K up to the melting point at 1406 K. It is mechanically unstable at 0 K with a negative shear constant $C' = (C_{11} - C_{12})/2$ around -35 GPa [35]. This behavior is similar to some transition metals which adopt the bcc structure only at high temperature before the melting as titanium [36,37]. The phonon spectra calculated using DFPT ($T = 0$ K) presents several soft modes (see Fig. 4) around H, N, and Γ points. C' is related to the slope of the transversal branch with imaginary frequencies in the Γ-N [110] direction, and is therefore negative at 0 K as found previously with total energies of distorted unit cells [4,35]. Using AIMD and the TDEP method we can follow the evolution of the frequencies in temperature. At 300 K and at higher temperature we no longer observe any imaginary frequencies around the H point, the mode considerably hardens with temperature. Along the Γ-N direction, the frequencies increase with temperature but stay very low at the N point for the transverse branch T_1 corresponding to atomic motions in the [001] direction. We also observe the persistence of a softening of the other transverse branch T_2 with atomic motions in the [1$\bar{1}$0] direction around the Γ point, meaning that C' has a low value. We also stress that the bcc structure is mechanically unstable at 300 K since the the diagonal components of the stress tensor diverge from each other, while at 900 K and above, the bcc structure becomes mechanically stable.

We present in Fig. 5 the evolution of the phonon frequencies of γ-U in pressure at 1600 K. All the frequencies increase as a function of pressure as for the α structure except for the transverse branch T_2 which softens with pressure close to the Γ point. So if temperature stabilizes the bcc structure, pressure has the opposite effect and destabilizes the bcc structure.

As for α-U we have extracted the elastic constants of the γ structure at the thermodynamic conditions of our molecular dynamics calculations. The evolution in pressure and temperature of K, G, and C' are presented in Fig. 6. At 0 GPa and 1000 K we found an equilibrium volume of 21.6 Å^3 and a bulk modulus of 105 GPa, close to the experimental value of 113 GPa reported by Yoo *et al.* [21]. As for the α phase, K increases almost linearly with pressure with a negligible temperature dependence. The two structures have very close bulk modulus values (see the dashed line in Fig. 6). The bulk modulus of γ-U is larger by about 10%. G is also temperature independent contrary to α-U with values almost two times smaller than for α-U.

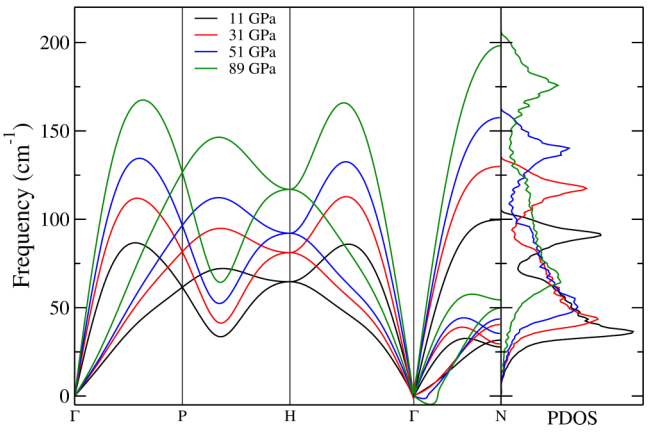

FIG. 5. Phonon dispersions and density of states for γ-U at 11, 31, 51, and 89 GPa and 1600 K.

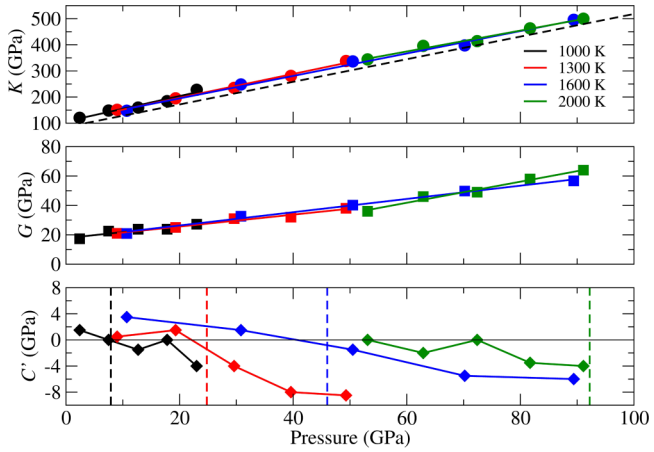

FIG. 6. Bulk modulus K, shear modulus G, and C' of γ-U as a function of pressure and at several temperatures. For K and G the symbols are the calculated values and the lines are linear fits of these values. The dashed line is a linear fit of the values of K for the α-U structure. For C' the dashed lines are the transition pressures between α and γ-U corresponding to each temperature.

C. Phase diagram of uranium

The huge variations of the γ and α-U phonon spectrum, when the temperature increases, sign the presence of strong anharmonic effects in the uranium material. Indeed, when the quasiharmonic approximation (QHA) applies, this means that all the temperature effects could be included in the thermal expansion. Conversely, this implies that no variation of the phonon spectrum can be obtained without any change of the volume. In this work, for isochoric simulations, the spectrum varies strongly as a function of temperature. Thus, the QHA cannot be applied definitively and the description of the uranium material needs to include explicit temperature effects, going beyond the QHA. That is what we performed in the present work.

Starting from the phonon spectrum and the corresponding phonon densities of states (PDOS) at various pressures and temperatures of α and γ-U, we can calculate the vibrational entropies and build the Gibbs free energies to find the transition line. We present in Fig. 7 the free energies $F = U - TS_{\text{vib}}$ for the volumes and temperatures considered in AIMD. These free energies are fitted with a Birch-Murnaghan equation of state to obtain the pressure and therefore the Gibbs energies. The transition pressures are obtained at each temperature when the Gibbs energies of the two structures are equal to each other. The resulting α/γ phase boundary is presented in Fig. 8 in comparison with experimental phase diagram of uranium [21]. We also present the volume change in the transition as a function of pressure with the experimental data [21].

The limit of the line transition at 0 GPa gives a transition temperature equal to 870 K, close to the experimental value of 940 K (α/β phase transition) and 1050 K (β/γ phase transition). Note that the intermediate β phase of uranium is not taken into account in present calculations. As a function of pressure, transition temperatures shown in Fig. 8 are about 300 K lower than the experimental ones. A possible source of errors responsible for this discrepancy might be the cell parameters of the orthorhombic α structure which are kept

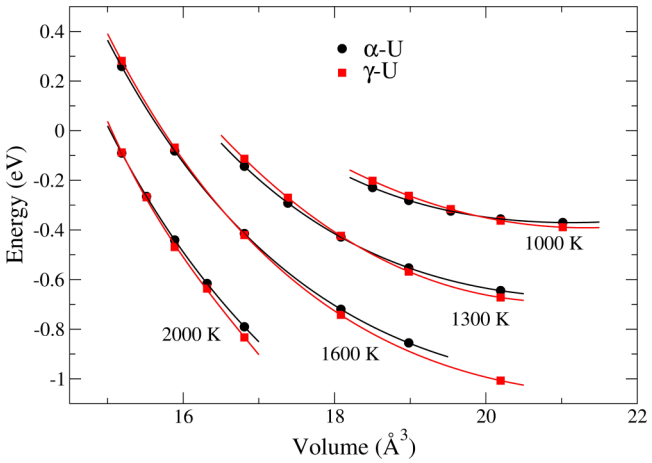

FIG. 7. Free energies for α and γ-U as a function of temperature and volume.

fixed to those obtained at 0 K during the AIMD simulations (whatever the temperature used). Thus, the α structure is clearly destabilized, its free energy is overestimated, and as a consequence the α/γ phase boundary is lowered. To test this hypothesis, we have performed calculations with optimized cell parameters at 1600 K and 90 GPa. This lowers the vibrational entropy by about 1 meV and then the transition pressure decreases by 2 GPa and the temperature increases by only 30 K. From the experimental part, the temperature gradients due to the laser heating from only one side of the sample and due to the spot size of the x-ray beam could also explain the discrepancy. In fact the authors [21] estimate their temperature uncertainties to 10%, so between 100 and 200 K depend on the pressure transition. It would be interesting to perform new experiments to take the benefits of the new setups with better focused x rays and laser heating on both sides of the sample [36].

Interestingly, this transition line, obtained by means of thermodynamical calculations is in good agreement with the

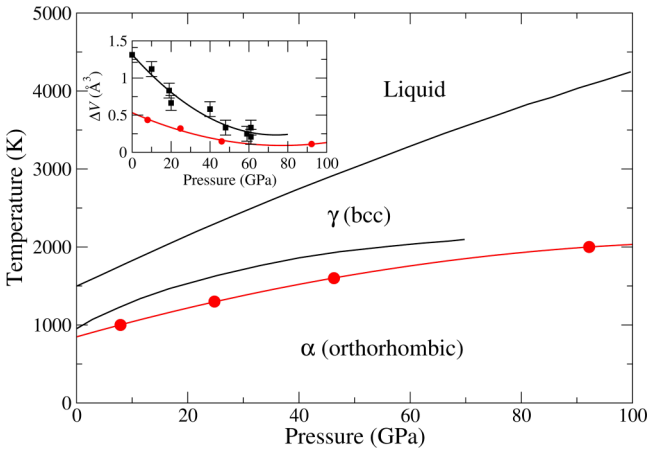

FIG. 8. Phase diagram of uranium. The black lines are the experimental transition lines [21] and the red circles are our results for the α-γ phase boundary. The inset shows the experimental (squares) and our theoretical (circles) volume changes in α-γ transitions as a function of pressure.

one expected from mechanical considerations. In Fig. 6 we have reported the pressure behavior of the elastic constant C' (solid lines) and the transition pressures between α and γ-U (dashed lines). When this constant is negative, the bcc structure is mechanically unstable. Despite the fact that C' oscillates because of its small values, it is remarkable that it becomes negative almost at the transition pressure. At 2000 K, C' stays close to zero. This is certainly due to the fact that the slope of the transition line becomes very small and that at this temperature and in this range of pressure we are close to the phase transition.

At low pressure we obtain large discrepancies with the experimental data [21] for the volume change, see the inset of Fig. 8. We found a jump of 0.5 Å^3 between the α and γ structure, while experimentally the value is around 1.3 Å^3. Accordingly, we do not reproduce the strong curvature of the α/γ phase boundary at low pressure. If we rule out the possibility of a problem in experiments, it is possible than this jump in volume comes from electronic correlations effects not taken into account in the present simulations. In fact, in close elements in the periodic table, namely cerium and plutonium, the electronic correlations increase with temperature and localize the electrons [38–40]. This phenomena is responsible for spectacular jumps of the equilibrium volumes, and to large discrepancies between calculations taken into account, or not, the electronic correlations. It is therefore possible that the $5f$ electrons of uranium becomes partially localized at high temperature and induced a volume jump at the phase transition. It would therefore be necessary to go beyond standard DFT calculations and use a method as the DFT+U as already proposed by Xie *et al.* [41].

Finally, *ab initio* calculations predict that the bct structure (the ground state of Pa) is less stable than the α phase but more stable that the γ phase [4,7] at 0 K. So, it would be possible to see a stabilization of this structure before the γ one when the temperature increases. We have performed simulations at 1000 and 2000 K with the bct structure. Its free energy is systematically higher than the α and γ ones and it is unlikely that this structure is adopted by uranium in the pressure and temperature range presented here.

IV. CONCLUSIONS

In this work we have explored the phase diagram of uranium up to 100 GPa and 2000 K by means of AIMD simulations. Using an homemade TDEP post-process, we have extracted the phonon spectra of the α and γ phases and have shown that strong anharmonic effects are present in this material. On one hand, the soft mode of the α phase hardens as a function of temperature (as mentioned in a previous work) unveiling a stabilization of this phase. However, this soft mode lasts at high temperature (900 K), disclosing that the thermodynamic properties of this phase remains affected by the CDW, even at high temperature. The decreasing of the shear modulus as a function of the temperature is probably related to this feature. On the other hand, the γ phase (which is not stable at 0 K) becomes mechanically stable above 900 K. Taking into account the experimental and theoretical uncertainties we find a good agreement between theory and experiments for the α/γ phase boundary.

The AIMD+TDEP method shows good performance to reproduce the phase diagram of uranium but also to predict the temperature- and pressure-dependent elastic properties. It would be interesting to pursue this study for other actinides, with even more complex phases diagrams (such as plutonium), in order to confirm the power of such a method but also to infer from phonon spectra the stabilization or transition mechanisms brought into play in actinide materials.

ACKNOWLEDGMENT

We would like to thank G. Weck for helpful discussions.

[1] D. Young, *Phase Diagram of the Elements* (University of California Press, Berkeley, CA, 1991).
[2] A. Lindbaum, S. Heathman, T. L. Bihan, R. Haire, N. Idiri, and G. Lander, J. Phys.: Condens. Matter **15**, S2297 (2003).
[3] S. Heathman, R. G. Haire, T. Le Bihan, A. Lindbaum, K. Litfin, Y. Méresse, and H. Libotte, Phys. Rev. Lett **85**, 2961 (2000).
[4] P. Söderlind, Adv. Phys. **47**, 959 (1998).
[5] X. Dai, S. Savrasov, G. Kotliar, A. Migliori, H. Ledbetter, and E. Abrahams, Science **300**, 953 (2003).
[6] J. M. Wills and O. Eriksson, Phys. Rev. B **45**, 13879 (1992).
[7] N. Richard, S. Bernard, F. Jollet, and M. Torrent, Phys. Rev. B **66**, 235112 (2002).
[8] J. Bouchet, R. C. Albers, M. D. Jones, and G. Jomard, Phys. Rev. Lett **92**, 095503 (2004).
[9] J. Bouchet and R. Albers, J. Phys.: Condens. Matter **23**, 215402 (2011).
[10] S. Baroni, S. de Gironcoli, and A. D. Corso, Rev. Mod. Phys. **73**, 515 (2001).
[11] J. Bouchet, F. Jollet, and G. Zerah, Phys. Rev. B **74**, 134304 (2006).
[12] J. Bouchet, Phys. Rev. B **77**, 024113 (2008).
[13] S. Raymond, J. Bouchet, G. H. Lander, M. Le Tacon, G. Garbarino, M. Hoesch, J.-P. Rueff, M. Krisch, J. C. Lashley, R. K. Schulze, and R. C. Albers, Phys. Rev. Lett. **107**, 136401 (2011).
[14] R. A. Reese, S. K. Sinha, and D. T. Peterson, Phys. Rev. B **8**, 1332 (1973).
[15] W. P. Crummett, H. G. Smith, R. M. Nicklow, and N. Wakabayashi, Phys. Rev. B **19**, 6028 (1979).
[16] A. Dewaele, J. Bouchet, F. Occelli, M. Hanfland, and G. Garbarino, Phys. Rev. B **88**, 134202 (2013).
[17] P. Söderlind, B. Grabowski, L. Yang, A. Landa, T. Björkman, P. Souvatzis, and O. Eriksson, Phys. Rev. B **85**, 060301 (2012).
[18] O. Hellman, I. A. Abrikosov, and S. I. Simak, Phys. Rev. B **84**, 180301 (2011).
[19] O. Hellman, P. Steneteg, I. A. Abrikosov, and S. I. Simak, Phys. Rev. B **87**, 104111 (2013).

[20] J. Bouchet and F. Bottin, Phys. Rev. B **92**, 174108 (2015).
[21] C.-S. Yoo, H. Cynn, and P. Söderlind, Phys. Rev. B **57**, 10359 (1998).
[22] The ABINIT code is a common project of the Catholic University of Louvain (Belgium), Corning Incorporated, CEA (France) and other collaborators, http://www.abinit.org.
[23] X. Gonze, B. Amadon, P.-M. Anglade, J.-M. Beuken, F. Bottin, P. Boulanger, F. Bruneval, D. Caliste, R. Caracas, M. Côté, T. Deutsch, L. Genovese, P. Ghosez, M. Giantomassi, S. Goedecker, D. Hamann, P. Hermet, F. Jollet, G. Jomard, S. Leroux, M. Mancini, S. Mazevet, M. Oliveira, G. Onida, Y. Pouillon, T. Rangel, G.-M. Rignanese, D. Sangalli, R. Shaltaf, M. Torrent, M. Verstraete, G. Zerah, and J. Zwanziger, Comput. Phys. Commun. **180**, 2582 (2009).
[24] P. E. Blöchl, Phys. Rev. B **50**, 17953 (1994).
[25] M. Torrent, F. Jollet, F. Bottin, G. Zerah, and X. Gonze, Comput. Mater. Sci. **42**, 337 (2008).
[26] J. P. Perdew, K. Burke, and M. Ernzerhof, Phys. Rev. Lett **77**, 3865 (1996).
[27] N. Holzwarth, A. Tackett, and G. Matthews, Comput. Phys. Commun. **135**, 329 (2001).
[28] ATOMPAW is a general license public code developed at Wake Forest University. Some of its capabilities have been developed at the Commissariat à l'énergie atomique, http://pwpaw.wfu.edu.
[29] A. Dewaele, M. Torrent, P. Loubeyre, and M. Mezouar, Phys. Rev. B **78**, 104102 (2008).
[30] F. Bottin, S. Leroux, A. Knyazev, and G. Zérah, Comput. Mater. Sci. **42**, 329 (2008).
[31] G. H. Lander, E. S. Fisher, and S. D. Bader, Adv. Phys. **43**, 1 (1994).
[32] L. T. Llyod and C. S. Barrett, J. Nucl. Mater. **18**, 55 (1966).
[33] E. S. Fisher, J. Nucl. Mater. **18**, 39 (1966).
[34] G. Simmons and H. Wang, *Single Crystal Elastic Constants and Calculated Aggregate Properties: A Handbook* (The MIT Press, Cambridge, MA, 1971).
[35] B. Beeler, C. Deo, M. Basker, and M. Okuniewski, J. Nucl. Mater. **433**, 143 (2013).
[36] A. Dewaele, V. Stutzmann, J. Bouchet, F. Bottin, F. Occelli, and M. Mezouar, Phys. Rev. B **91**, 134108 (2015).
[37] C.-E. Hu, Z.-Y. Zeng, L. Zhang, X.-R. Chen, L.-C. Cai, and D. Alfè, J. Appl. Phys. **107**, 093509 (2010).
[38] B. Amadon, S. Biermann, A. Georges, and F. Aryasetiawan, Phys. Rev. Lett **96**, 066402 (2006).
[39] B. Amadon, Phys. Rev. B **94**, 115148 (2016).
[40] J. Bouchet, B. Siberchicot, F. Jollet, and A. Pasturel, J. Phys.: Condens. Matter **12**, 1723 (2000).
[41] W. Xie, W. Xiong, C. A. Marianetti, and D. Morgan, Phys. Rev. B **88**, 235128 (2013).